Kinetic-energy operator in the effective shell-model interaction

L. Jaqua
Department of Physics, University of Arizona, Tucson, Arizona 85721

M. A. Hasan
Applied Science University, Amman, Jordan

J. P. Vary
Department of Physics and Astronomy, Iowa State University, Ames, Iowa 50011

B. R. Barrett
Department of Physics, University of Arizona, Tucson, Arizona 85721
(Received 14 July 1992)

Differences in the Hartree-Fock and effective shell-model interaction arising from alternative treatments of the kinetic-energy operator in finite nuclear many-body problems are described. The Hartree-Fock single-particle energies and their relationship to experimental removal energies depend sensitively on whether or not the center-of-mass kinetic energy is retained in the nuclear Hamiltonian. Large effects in particle-hole energies are obtained which have important consequences for effective shell-model Hamiltonians. If the center-of-mass contribution of the kinetic-energy operator is removed from the Hamiltonian, substantial effects appear in a simple example of the shell-model spectra of ^{16}O and ^{17}O treated as four and five valence nucleons, respectively, outside a ^{12}C core. The contributions to the energy coming from the valence, relative kinetic-energy operator push the energy spectra of both nuclei up by about 1 MeV relative to their ground states.

PACS number(s): 21.60.Cs, 21.10.−k, 27.20.+n

I. INTRODUCTION

It has long been recognized that the nuclear shell model is affected in two ways by spurious center-of-mass motion (see, for example, Refs. [1]–[7]). First, by describing any state of A nucleons in terms of Slater determinants of A single-particle (sp) states, one is specifying a wave function for the center-of-mass (c.m.) motion. In so far as this c.m. motion is different in different states of the A-particle system, the effects on spectra, transition rates, etc., can be highly nontrivial [2]–[7]. For this reason, considerable effort has been devoted to developing methods of projecting out or constraining the c.m. wave function [4]–[7]. Second, by defining the nuclear Hamiltonian to have a sum of A one-body kinetic-energy operators, one includes the c.m. kinetic energy in the energy of each state [6]. This effect could be treated perturbatively in any state by simply subtracting the expectation value of the c.m. kinetic-energy operator from the Hartree-Fock (HF) energy [8] or from the shell-model eigenvalue [3]. The main point of the present effort is to show that a nonperturbative treatment of the role of the c.m. kinetic-energy operator leads to substantial effects in the energy spacings of shell-model states. We do not address here the very interesting, but separate, issue of c.m. motion in the nuclear wave function, since this has already been extensively investigated [2]–[7].

We begin by noting that the simplest conventional nuclear Hamiltonian is written as a sum of the one-body kinetic-energy operators, T_i, and the interactions between the nucleons V_{ij}. In other words

$$H' = \sum_{i=1}^{A} T_i + \sum_{i<j}^{A} V_{ij} \equiv T + V \ . \tag{1}$$

Just as T, for a two-body system, can be rewritten as a sum of relative and c.m. kinetic energies, we can rewrite T for A particles as

$$T = T_{\rm rel} + T_{\rm c.m.} \tag{2}$$

with

$$T_{\rm c.m.} = \frac{1}{2Am}\left(\sum_{i=1}^{A} \mathbf{p}_i\right)^2 , \tag{3}$$

and

$$T_{\rm rel} = \frac{2}{A}\sum_{i<j}^{A} \frac{\mathbf{p}_{ij}^2}{2\mu} \equiv \sum_{i<j}^{A} T_{ij}, \tag{4}$$

where

$$\mathbf{p}_{ij} = \frac{(\mathbf{p}_i - \mathbf{p}_j)}{2}, \tag{5}$$

$\mu = m/2$ and m is the nucleon mass, for both neutrons and protons. Thus H' contains $T_{\rm c.m.}$ as a consequence of having a simple, one-body, form of T. Here we investigate

the changes in HF calculations and in shell-model spectra which result from removing $T_{\text{c.m.}}$ from H' leaving

$$H = T_{\text{rel}} + V = \sum_{i<j}^{A} \left(\frac{\mathbf{p}_{ij}^2}{A\mu} + V_{ij} \right) . \tag{6}$$

To start with H, a pure two-body operator, and derive an effective shell-model interaction following the theory of Brueckner and co-workers [9,10], Bethe and Goldstone [11], and Brandow [12] and using a realistic nucleon-nucleon interaction would comprise a significant research undertaking. Therefore, for these initial demonstrations, treating the interactions as static nucleon-nucleon potentials V_{ij}, we will employ previously calculated effective interactions and simply look at the approximate nonperturbative effects of subtracting $T_{\text{c.m.}}$ from H'.

II. ELIMINATION OF $T_{\text{c.m.}}$ FROM HARTREE-FOCK

We first investigate the HF problem before studying its effects on shell-model calculations. Starting with H as given in Eq. (6) one may solve the nuclear HF problem along traditional lines [8], as was first done in Ref. [13]. Some of the important consequences of this choice of H for the interpretations of the sp energies and for corrections to HF have been discussed [14]. It is our intention to review the salient issues at the HF level and later to outline the consequences for effective shell-model interactions as well as for the resulting shell-model spectra.

Next we note that one can also write H in the form

$$H = \left(1 - \frac{1}{A}\right) \sum_{i=1}^{A} T_i + \sum_{i<j}^{A} \left(V_{ij} - \frac{\mathbf{p}_i \cdot \mathbf{p}_j}{mA} \right), \tag{7}$$

where a one-body operator is still manifest. The HF treatment of this form has been shown to yield the same solution as the HF treatment of Eq. (6) to within a unitary transformation among the occupied orbitals [15]. Although the HF solutions of Eqs. (6) and (7) are simply related, it is important to note that the HF Hamiltonian's sp wave functions and sp energies are different for each form of H as well as being nontrivially different from those obtained in the HF solutions of H', Eq. (1). It is our intention here to follow the consequences for the HF and shell-model problems that emerge from the choice of Eq. (6) for the Hamiltonian rather than the conventional choice of H' in Eq. (1). To the extent that these differences are significant, we motivate a future effort to employ Eq. (7) in a similar study.

For V_{ij} we select an effective interaction developed [16] from the Reid soft core nucleon-nucleon interaction [17] specifically for applications, such as HF calculations, in very large model spaces. This effective interaction is obtained in a harmonic-oscillator basis with $\hbar\Omega = 14.0$ MeV and this same basis is employed throughout the calculations we report here. Improvement of this effective interaction in the form of a folded-diagram correction, which we include here, and applications within thermal HF have been described previously [18]. We evaluate the HF results for ^{16}O in a basis of the lowest six oscillator shells as a function of a strength parameter, λ, multiplying V_{ij}. We also include the two-body Coulomb interaction between protons. In summary, the two Hamiltonians whose results we compare through HF are

$$H'_\lambda = T + \lambda V + V_C \tag{8}$$

and

$$H_\lambda = T_{\text{rel}} + \lambda V + V_C. \tag{9}$$

We will use the convention that normally occupied (unoccupied) orbitals are signified by capital (lower case) Roman letters. Greek letters are used to signify all possible states. In the case of H'_λ the HF energy is expressed in terms of the sp energies ϵ'_A, such that

$$E'_{\text{HF}} = \sum_A [\epsilon'_A - \tfrac{1}{2}\langle A \mid U \mid A\rangle], \tag{10}$$

which can also be written as

$$E'_{\text{HF}} = \frac{1}{2} \sum_A [\epsilon'_A + \langle A \mid T \mid A\rangle]. \tag{11}$$

The usual mean-field potential, $\langle A \mid U \mid A\rangle$, is given by

$$\langle A \mid U \mid A\rangle = \sum_B \langle AB \mid H'_\lambda \mid AB\rangle. \tag{12}$$

On the other hand, for H_λ, the HF energy is

$$E_{\text{HF}} = \frac{1}{2} \sum_A \epsilon_A. \tag{13}$$

One can think that the form of E_{HF} in Eq. (13) emerges from E'_{HF} in Eq. (11) when we proceed from H'_λ to H_λ and omit the one-body operators from the nuclear Hamiltonian.

Within HF one usually obtains first the "HF rms radius" based on the A self-consistent sp wave functions with point nucleons and then applies two corrections to compare with the measured charge radius in light nuclei. However, the corrections to the HF rms radius for the finite charge distribution of the proton and the c.m. motion of the nucleus largely cancel in a light nucleus such as ^{16}O [19]. Thus, we may, to a very good approximation, compare the HF rms radius without corrections with the measured charge radius of 2.71 fm in ^{16}O [20]. For this reason, we simply employ the HF rms radius in the presentation of our results.

The HF energies and rms radii are evaluated for each Hamiltonian at selected values of λ and the results are plotted in Fig. 1. Experimentally the point-mass rms radius for ^{16}O is 2.59 fm [20] and the binding energy is 127.617 MeV [21]. Note that for $\lambda = 1.0$ the results for H'_λ are reminiscent of the Brueckner-Hartree-Fock results obtained earlier for ^{16}O [22]. That is, there is significant underbinding while the rms radius, before correction for spurious c.m. motion in the wave function, is in rough accord with the point-mass radius deduced from experiment [20].

There is a systematic difference between E_{HF} (short

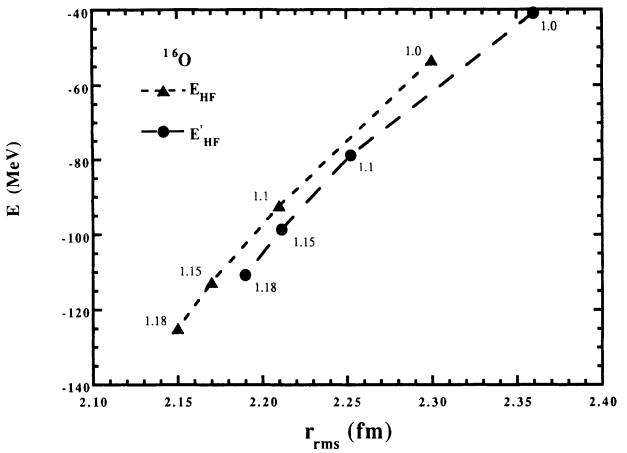

FIG. 1. Hartree-Fock energy ($E_{\rm HF}$ and $E'_{\rm HF}$) vs rms radius for ^{16}O in a six-major-oscillator-shell calculation as a function of the two-body interaction strength λ. The values of λ are indicated close to the corresponding point for each of the Hamiltonians considered.

dashed line) and $E'_{\rm HF}$ (long dashed line) which is primarily accounted for by evaluating the perturbative correction and showing that

$$E_{\rm HF} \approx E'_{\rm HF} - \langle T_{\rm c.m.}\rangle', \tag{14}$$

where the prime signifies taking the expectation value with respect to the HF solutions to H'_λ. In fact since

$$H'_\lambda = H_\lambda + T_{\rm c.m.} \tag{15}$$

it follows that

$$E'_{\rm HF} = \langle H'_\lambda\rangle = \langle H_\lambda + T_{\rm c.m.}\rangle' \geq \langle H_\lambda\rangle + \langle T_{\rm c.m.}\rangle'. \tag{16}$$

The inequality arises since the HF solution for H_λ is, by definition, the minimum-expectation value of H_λ. Clearly, the perturbative correction to $E'_{\rm HF}$ will leave the corrected HF energy above $E_{\rm HF}$. That is

$$E_{\rm HF} \leq E'_{\rm HF} - \langle T_{\rm c.m.}\rangle'. \tag{17}$$

The differences in the rms radii are more interesting and more subtle. To our knowledge, these rather sizable differences have not been noted in the literature. These differences indicate that the presence of $T_{\rm c.m.}$ in the nuclear Hamiltonian has a significant impact on the HF wave function, since it increases the rms mass radius by an amount between 0.04 and 0.06 fm in ^{16}O. Reading from the curves in Fig. 1, to get an impression of the significance of this result, we see that it takes about a 5% reduction in the strength of λV_{ij} to accomplish the same rms-mass-radius change for a given choice of the Hamiltonian. These differences in the HF wave functions may be expected to have significant effects on shell-model spectra as well, and we will consider these effects in another effort [23]. Here, however, we will discuss the consequences of the different definitions of the Hamiltonian and the different HF sp energies on the results obtained for the shell-model problem.

III. EFFECTS ON HARTREE-FOCK SINGLE-PARTICLE SPECTRA AND WAVE FUNCTIONS

Let us look at the HF sp energies ϵ'_A and ϵ_A as shown in Table I for ^{16}O with $\lambda = 1.18$. The occupied HF states from H'_λ are $20 - 22$ MeV more bound than those from H_λ while the unoccupied states are about 24 MeV more bound. These differences for the occupied states are, to a rough approximation, the consequences of Eqs. (11), (13), and (17). If we put these equations together and approximate the differences between ϵ'_B and ϵ_B as being state independent, we obtain

$$\epsilon_B \approx \epsilon'_B + \left(\langle B \mid T \mid B\rangle - \frac{1}{A}\langle T_{\rm c.m.}\rangle\right) \tag{18}$$

and

$$\epsilon_B \approx \epsilon'_B + \frac{1}{A}\langle T_{\rm rel}\rangle. \tag{19}$$

Now, in the harmonic-oscillator ground state ($\hbar\Omega = 14.0$ MeV), ^{16}O has $\langle T_{\rm c.m.}\rangle = 10.5$ MeV, $\langle T\rangle = 252$ MeV, and $\langle T_{\rm rel}\rangle = 241.5$ MeV, which implies an estimate for $\frac{1}{A}\langle T_{\rm rel}\rangle = 15.1$ MeV. The larger effects actually observed are primarily a consequence of the smaller rms radius of the HF solution at $\lambda = 1.18$, compared with the pure oscillator with $\hbar\Omega = 14.0$ MeV .

Since our goal is to examine the consequences of selecting H_λ instead of H'_λ for the basis of a theory of the shell model, we examine the sp spectra more closely. Let us recall Koopmans' theorem [24] which assumes the self-consistent fields are the same for the A and the $(A-1)$ systems and then states that the removal energy for a particle in state B is the same as the HF sp energy

$$E'_{\rm HF} - E'_{\rm HF}(B \text{ removed}) = \epsilon'_B. \tag{20}$$

In the spirit of this result one assumes these rearrangement effects are small and compares the HF sp energies with the experimental removal energies. Implicit in Koopmans' theorem is the use of the A-independent form of the Hamiltonian, H', of Eq. (1). The use of H_λ, Eq. (6), leads to a state-dependent correction [15]

$$E_{\rm HF} - E_{\rm HF}(B \text{ removed}) = \epsilon_B - \frac{1}{A-1}\sum_{C\neq B}\sum_{D}\langle CD \mid T_{\rm rel} \mid CD\rangle \tag{21}$$

and implies that the sp energies ϵ_α are not directly comparable with the experimental removal energies. If we use

TABLE I. Hartree-Fock energies $\lambda = 1.18$.

	$\epsilon_\alpha{}'$		ϵ_α	
	n	p	n	p
$0s_{1/2}$	-66.78	-62.01	-44.98	-40.25
$0p_{3/2}$	-32.28	-28.22	-12.67	-8.57
$0p_{1/2}$	-21.05	-16.96	-0.74	3.37
$0d_{5/2}$	-4.24	-0.50	19.62	23.40
$1s_{1/2}$	-1.42	2.02	22.39	25.86
$0d_{3/2}$	5.27	8.64	29.21	32.57

TABLE II. Neutron wave functions.

	$H_{\rm HF}'$			$H_{\rm HF}$		
	n = 0	n = 1	n = 2	n = 0	n = 1	n = 2
$0s_{1/2}$	-0.9621	-0.2650	-0.0644	-0.9637	-0.2596	-0.0621
$0p_{3/2}$	0.9613	0.2615	0.0867	0.9532	0.2874	0.0937
$0p_{1/2}$	-0.9783	-0.1865	-0.0907	0.9716	0.2158	0.0969
$0d_{5/2}$	0.9887	0.1500		-0.9883	-0.1525	
$1s_{1/2}$	0.2643	-0.9643	0.0181	-0.2581	0.9656	-0.0320
$0d_{3/2}$	0.9901	-0.1400		-0.9869	0.1611	

the additional approximation of Eq. (14) together with Eqs. (20) and (21), we obtain another potentially useful relation

$$\epsilon_B' \approx \epsilon_B - \frac{1}{A-1}\sum_{C\neq B}\sum_{D}\langle CD \mid T_{\rm rel} \mid CD\rangle. \qquad (22)$$

For purposes of using HF as the starting point of a microscopic many-body theory, the differences between the sp energies of the occupied and unoccupied states are of central importance. Insofar as the shift between ϵ_α and ϵ_α' is a state-independent quantity, as the approximation in Eq. (18) suggests, then differences between sp energies are unaffected and there are no consequences for effective shell-model interactions. However, the residual state-dependence leads to substantial changes in the particle-hole (p-h) energies. For example, the neutron $1d_{5/2}$-$1p_{1/2}$ spacing is 16.8 MeV arising from H_λ', while it is 20.4 MeV arising from H_λ. In general, all the p-h spacings are $1-4$ MeV larger for ϵ_α than for ϵ_α'.

Now, let us consider the self-consistent sp wave functions for the $\lambda = 1.18$ HF results. We already expect some differences between the HF orbitals obtained from H_λ' and H_λ in view of the differences in rms radii depicted in Fig. 1. We present in Tables II and III the amplitudes for the occupied and lowest-lying unoccupied HF orbitals in the harmonic-oscillator basis for H_λ' and H_λ. While these amplitudes exhibit, as might be expected, a healthy mixing of the oscillator states used to describe the HF orbitals, there are only small differences evident between the HF states of H_λ' and the corresponding states of H_λ.

IV. CONSEQUENCES FOR THE EFFECTIVE SHELL-MODEL INTERACTION

How the above calculated differences in p-h energies and sp wave functions affect other observables in a full microscopically derived shell model will be investigated further in a future publication [23]. At present we prefer to outline the formal consequences for the shell model emanating from the selection of $H = T_{\rm rel} + V$, rather than $H' = T + V$, and to provide schematic calculations that indicate the scale of differences that may emerge in the shell-model spectra.

Let us signify by H_0 the HF Hamiltonian resulting from H. The HF sp states, $\mid \alpha\rangle$,are solutions of

$$H_0 \mid \alpha\rangle = \epsilon_\alpha \mid \alpha\rangle. \qquad (23)$$

The HF energy, $E_{\rm HF}$, is given by Eq. (13). There are a number of ways we could proceed to define a shell-model problem. In analogy with the usual procedure of adding and subtracting the self-consistent potential U, we will add and subtract the self-consistent H_0,

$$H = H_0 + [H - H_0] \qquad (24)$$

and we treat the "residual" interaction $H - H_0$ as the source of our effective shell-model interaction. Immediately, one notices a very important consequence of this choice of the residual interaction when one works in the self-consistent basis $\{\mid \alpha\rangle\}$: The usual cancellation of sp insertions is achieved in a particularly simple way expressed by the diagram elements shown in Fig. 2 since the basis is the eigenbasis of H_0. The vast majority of sp insertions vanish altogether. The surviving diagonal insertions (which still cancel in pairs) are equal in magnitude to HF sp energies.

The usual linked, folded-diagram expansion for the effective shell-model interaction (see, for example, Ref. [25]) may be carried out starting from Eq. (6). Using the basis, $\{\mid \alpha\rangle\}$, the expansion is free of diagrams with insertions and the conventional Brueckner-Bethe-Goldstone-

TABLE III. Proton wave functions.

	$H_{\rm HF}'$			$H_{\rm HF}$		
	n = 0	n = 1	n = 2	n = 0	n = 1	n = 2
$0s_{1/2}$	0.9652	0.2549	0.0599	0.9666	0.2498	0.0570
$0p_{3/2}$	0.9653	0.2480	0.0822	0.9569	0.2763	0.0895
$0p_{1/2}$	0.9825	0.1644	0.0876	0.9757	0.1979	0.0936
$0d_{5/2}$	-0.9921	-0.1252		0.9921	0.1257	
$1s_{1/2}$	-0.2519	0.9663	-0.0529	-0.2457	0.9668	-0.0699
$0d_{3/2}$	0.9848	-0.1739		0.9804	-0.1968	

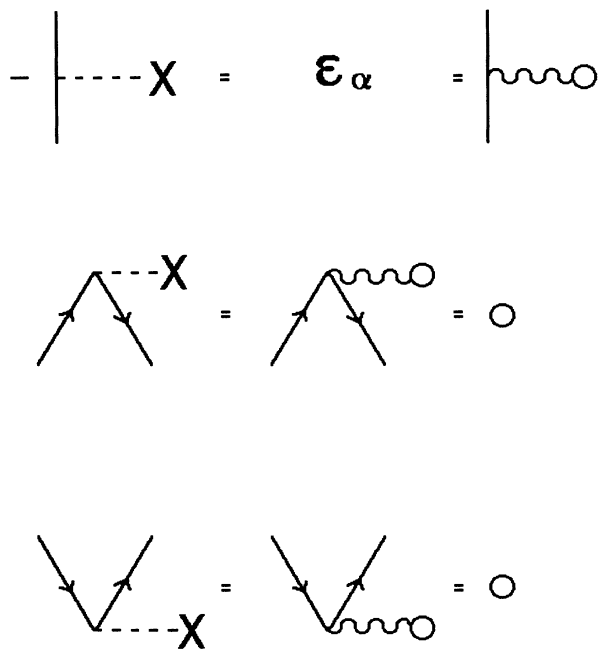

FIG. 2. The simple values for insertions that emerge when $H - H_0$ is chosen for the residual interaction and when one employs the self-consistent basis generated by H_0. We employ dashed lines with a terminating "X" to represent insertions of $-H_0$ and wavy lines to signify the two-body operator H. Lines drawn without arrows indicate either particle lines or hole lines. Note that there is a minus sign before the $-H_0$ insertion so that the net result is $+\epsilon_\alpha$. In addition, note that all off-diagonal insertions on particle lines and hole lines vanish.

Brandow theory [9]–[12] can be implemented with

$$\bar{V} = T_{\rm rel} + V, \tag{25}$$

replacing the usual V in all expressions. This leads to the equation

$$G(\omega) = \bar{V} + \bar{V}\frac{Q^{2p}}{\omega - H_0}G(\omega), \tag{26}$$

where Q^{2p} is the two-particle Pauli operator and ω is the starting energy; and the effective interaction $\mathcal{V}_{\rm eff}$ can be written in terms of G as

$$\mathcal{V}_{\rm eff} = G + G\frac{Q'}{E_0^v - H_0^v}\mathcal{V}_{\rm eff}, \tag{27}$$

where it is understood that only the linked terms are retained. The unperturbed, self-consistent Hamiltonian for the valence particles is H_0^v, and E_0^v signifies the unperturbed valence energy. The operator Q' allows excitations into all intermediate states outside the valence model space, except for the two-particle ladder states already included in the calculation of G.

In subtracting $T_{\rm c.m.}$ from H' to get H, we first note that, once a core of i_c nucleons has been chosen, we can subdivide $T_{\rm rel}$ into

$$T_{\rm rel} = \sum_{i<j}^{i_c} T_{ij} + \sum_{i\le i_c<j}^{A} T_{ij} + \sum_{i_c<i<j}^{A} T_{ij} \equiv T_c + T_{\rm cv} + T_v, \tag{28}$$

where we have a core component T_c, a core-valence component $T_{\rm cv}$, and a valence component T_v. Following the usual path for the two-body effective interaction we argue that the contributions of T_c will be included in the core energy and the effects of $T_{\rm cv}$ will be included in the valence space sp energies.

V. INITIAL SHELL-MODEL APPLICATION

Our interest is focused on the role of T_v which appears in a similar capacity as the effective-residual interaction between the valence nucleons. We simplify the problem by selecting a sp shell-model space of harmonic-oscillator states instead of the full solutions to the HF problem [8], as described earlier. This is done to look for the predominant effects of treating the two-body character of the kinetic-energy operator and ignore the presumed smaller energy effects due to differences between oscillator and realistic sp wave functions in light nuclei.

By writing the kinetic-energy operator in the form of Eq. (2), we are able to remove its c.m. contribution exactly. Also, by writing the antisymmetrized wave functions only in terms of the relative coordinates, the spurious c.m. motion could, in principle, be completely removed from the calculated excitation energies. However, sp wave functions calculated with respect to a fixed potential are used and because these wave functions are written in the form of a Slater determinant to handle the antisymmetrization correctly, spurious c.m. effects are introduced into the calculated excitation energies. In the present calculations we do not address these spurious c.m. effects due to the wave functions which have been studied in Ref. [8], but concern ourselves with how the exact removal of the c.m. part of the kinetic-energy operator influences the calculated excitation energies.

We now follow the time-independent effective interaction approach [11,12,25] to second order in the Brueckner G matrix [9,10] to obtain an effective shell-model Hamiltonian given by Eq. (27). We begin by considering the G matrix itself written as

$$G = (T_v + V) + V\frac{Q^{2p}}{\omega - H_0}G + T_v\frac{Q^{2p}}{\omega - H_0}G. \tag{29}$$

(Note that T_v is the part of $T_{\rm rel}$ not involving core nucleons.) To obtain a first estimate of the size of the changes arising from our removal of the c.m. kinetic-energy term, we drop the last term in Eq. (29), arguing it is small compared to the third term, because T_v couples only to low-lying excited states, while V can also couple to high-lying excited states. We combine the second and third terms to form

$$G' = V + V\frac{Q^{2p}}{\omega - H_0}G. \tag{30}$$

Next we approximate G' as the solution of a Bethe-Goldstone equation

$$G' = V + V\frac{Q^{2p}}{\omega - H_0}G', \tag{31}$$

where G in Eq. (29) differs from G' by the term T_v. Thus we arrive at

$$G \cong T_v + G', \tag{32}$$

which embodies a major point of our development. We argue that one major effect of eliminating the spurious c.m. kinetic-energy operator from the development, in the fashion we have chosen, results, approximately, in T_v as an additive effective interaction term. Utilizing Eq. (32) in the role of the traditional Brueckner G matrix, working to second order in G, and maintaining only the leading-order term in T_v, we obtain

$$H_{\text{eff}} \cong T_v + G' + G'\frac{Q'}{E_0^v - H_0^v}G' \equiv T_v + \mathcal{V}_{\text{eff}}. \tag{33}$$

In the usual effective interaction theory the energy denominator in Eq. (33) is replaced with unperturbed oscillator energies. As our earlier HF calculations show, the differences between particle (unoccupied) and hole (occupied) energies can vary by up to 25%. Consequently, a more accurate investigation of $\mathcal{V}_{\text{eff}}$ should include this effect as well but we leave this study to a future effort.

With these approximations, we argue that the main difference in the effective shell-model interaction arising from the removal of $T_{\text{c.m.}}$ is the additive T_v term appearing in Eq. (33). Through our HF discussions it is clear that the sp energies are also different once $T_{\text{c.m.}}$ is removed. Our goal is then to compare shell-model spectra obtained with H_{eff} and with $\mathcal{V}_{\text{eff}}$ when sp energies are separately determined by fits to experimental spectra.

We now investigate the effect of removing $T_{\text{c.m.}}$ on the spectra of ^{16}O and ^{17}O. For simplicity, we will employ in Eq. (33) a similar $\mathcal{V}_{\text{eff}}$ [16, 18, 26] to that used in our HF calculations. The terms involving G' are taken to be a no-core G matrix [16,18] plus a folded-diagram correction [18] evaluated in an oscillator basis [16, 18, 26] with $\hbar\Omega =$ 14.0 MeV and with a starting energy of 9.0 MeV. The model space for $Q^{2p} = 0$ in this shell-model application is comprised of the lowest four oscillator shells ($0s_{1/2}$, $0p_{1/2}$, $0p_{3/2}$, $0d_{3/2}$, $0d_{5/2}$, $1s_{1/2}$, $1p_{1/2}$, $1p_{3/2}$, $0f_{5/2}$, $0f_{7/2}$).

It is sufficient for our purposes to demonstrate the differences in H_{eff} and $\mathcal{V}_{\text{eff}}$ in the the low-lying shell-model spectra of ^{16}O and ^{17}O, treated as four and five valence nucleons, respectively, outside a ^{12}C core. The valence space for our shell-model calculations consists of the $0p_{1/2}$, $0d_{5/2}$ and $1s_{1/2}$ sp orbitals. In order to account for the differences in the HF sp spectra, for the role of T_{cv}, and for neglected core-polarization effects, we separately adjust the single-particle spectra for H_{eff} and $\mathcal{V}_{\text{eff}}$. By adjusting the sp energies so that we fit the many-body spectra of the two nuclei in question, we might actually camouflage part of the net effects we are atttempting to examine.

The spectra are computed with the OXBASH shell-model code [27]. The results for the spectra of ^{16}O and ^{17}O are listed in Tables IV and V, respectively. Calculation 1 is performed with the interaction H_{eff}, fitting the lowest 3^-, 1^-, and 2^- states in ^{16}O and the $\frac{1}{2}^+$, $\frac{1}{2}^-$, and $\frac{5}{2}^-$ levels in ^{17}O, and using the sp energies $\epsilon(0d_{5/2})$ and $\epsilon(1s_{1/2})$ as adjustable parameters. In all calculations $\epsilon(0p_{1/2})$ is fixed at 0.0 MeV and the ^{16}O and ^{17}O spectra are shifted so the ground states are at zero energy. These same sp energies are then utilized in calculation 2 to determine the spectra of ^{16}O and ^{17}O, but now for the interaction $\mathcal{V}_{\text{eff}}$. Conversely, calculation 3 is done by fitting the above-mentioned states with the interaction $\mathcal{V}_{\text{eff}}$ and again by using the sp energies as adjustable parameters. This set of sp energies is then employed with H_{eff} to calculate the spectra of ^{16}O and ^{17}O, yielding the results of calculation 4.

In calculation 1 the best fit to experimental data yields sp energies of 8.50 and 4.75 MeV for the $0d_{5/2}$ and $1s_{1/2}$ states, respectively. Similarly, in calculation 3, where $\mathcal{V}_{\text{eff}}$ is fitted to the experimental spectra of ^{16}O and ^{17}O, the sp energies are $\epsilon(0d_{5/2}) = 9.00$ MeV and $\epsilon(1s_{1/2}) = 5.50$ MeV. For the reasons outlined above these sp energies should not be compared directly with experimental sp energies. However, in both cases the $0d_{5/2}$ sp energy value is higher than that of the $1s_{1/2}$ sp energy which is consistent with the experimental ordering. Note that this calculation is done with a ^{12}C core, and, experimentally, ^{13}C shows the $\frac{1}{2}^+$ state lying lower than the $\frac{5}{2}^+$ state by 0.76 MeV.

We notice that calculations 1 and 3 provide reasonably good fits for those states in the spectra of ^{16}O and ^{17}O, which are easily constructed within our model space. A 0^- intruder state appears in the calculated ^{16}O spectrum due to inadequacies of our simplified model and it is not listed for reasons of clarity. Likewise, the second experimental 0^+ and the first 2^+ states of ^{16}O are believed to be due to a coherent four-particle–four-hole excitation, are not well represented in our limited model space, and are, therefore, not listed.

Comparing the fit of calculation 1 with that of calculation 3, we note that, when the Hamiltonian contains the relative kinetic-energy operator (calculation 1), the excited states are "pushed" up relative to the ground state. In the limit of a closed core plus a single valence nucleon, this effect would be contained in the sp energies. Here, in the case of configuration mixing in the four- and five-

TABLE IV. ^{16}O spectra.

State	Experiment	H_{eff}[a]	$\mathcal{V}_{\text{eff}}$[b]	$\mathcal{V}_{\text{eff}}$[c]	H_{eff}[d]
0^+	0.00	0.00	0.00	0.00	0.00
3^-	6.13	6.39	5.35	5.72	6.81
1^-	7.12	7.08	6.19	6.79	7.73
2^-	8.87	8.84	7.79	8.17	9.26

[a]Fit H_{eff} with $\epsilon(1d_{5/2}) = 8.50$ MeV, $\epsilon(2s_{1/2}) = 4.75$ MeV.
[b]Calculation using $\mathcal{V}_{\text{eff}}$ with sp energies from [1].
[c]Fit $\mathcal{V}_{\text{eff}}$ with $\epsilon(1d_{5/2}) = 9.00$ MeV, $\epsilon(2s_{1/2}) = 5.50$ MeV.
[d]Calculation using H_{eff} with sp energies from [3].

TABLE V. ^{17}O spectra.

State	Experiment	H_{eff}[a]	$\mathcal{V}_{\text{eff}}$[b]	$\mathcal{V}_{\text{eff}}$[c]	H_{eff}[d]
$\frac{5}{2}^+$	0.00	0.00	0.00	0.00	0.00
$\frac{1}{2}^+$	0.87	0.25	-0.11	0.17	0.52
$\frac{1}{2}^-$	3.05	5.19	3.42	4.35	6.09
$\frac{5}{2}^-$	3.84	5.51	3.77	4.44	6.18

[a]Fit H_{eff} with $\epsilon(1d_{5/2}) = 8.50$ MeV, $\epsilon(2s_{1/2}) = 4.75$ MeV.
[b]Calculation using $\mathcal{V}_{\text{eff}}$ with sp energies from [1].
[c]Fit $\mathcal{V}_{\text{eff}}$ with $\epsilon(1d_{5/2}) = 9.00$ MeV, $\epsilon(2s_{1/2}) = 5.50$ MeV.
[d]Calculation using H_{eff} with sp energies from [3].

particle states, the effect arises because the different levels are "pushed" up by different amounts, so the excited states are more spread apart by T_v. This result appears in spite of the fact the sp energies are adjusted in each case to obtain a good fit to the experimental spectra.

The difference between the spectra for H_{eff} and $\mathcal{V}_{\text{eff}}$ for the same set of sp energies (i.e., calculations 1 and 2) shows on the average a 1.5 MeV effect, or about a 25% shift due to the role of T_v.

By fitting the ^{16}O and ^{17}O spectra with $\mathcal{V}_{\text{eff}}$ (calculation 3) and then using these new sp energies to calculate the spectra with H_{eff} (calculation 4), we show the same qualitative role of T_v.

VI. SUMMARY

In summary we have shown that the Hartree-Fock single-particle energies and their relationship to the experimental removal energies change dramatically when the c.m. kinetic-energy operator is removed from the Hamiltonian. We have also shown that the differences in the spectra of ^{16}O and ^{17}O by omitting $T_{\text{c.m.}}$ and treating the resulting T_v as part of the two-body interaction, are of the form of a positive additive shift of the spectrum away from the ground state on the order of 20–25%. These effects merit a more extensive study, where one, for example, includes T_{rel} along with the nulceon-nucleon interaction in the calculation of the Brueckner G matrix as indicated in Eqs. (25) and (26).

The authors would like to thank E. David Davis for helpful discussions and to acknowledge partial support of this work by the National Science Foundation, Grant No. PHY-9103011, INT-9215017, and by the Department of Energy, Division of High Energy and Nuclear Physics Grant No. DE-FG02-87ER40371.

[1] J. P. Elliott and T. H. R. Skyrme, Proc. R. Soc. London, Ser. A **232**, 561 (1955).
[2] S. Gartenhaus and C. Schwartz, Phys. Rev. **108**, 482 (1957).
[3] E. Baranger and C. W. Lee, Nucl. Phys. **22**, 157 (1961).
[4] R. M. Dreizler, F. R. Krejs, and A. Klein, Nucl. Phys. **A155**, 33 (1970).
[5] D. J. Ernst, C. M. Shakin, and R. M. Thaler, Phys. Rev. C **7**, 925 (1973); **8**, 440 (1973).
[6] H. G. Miller and J. P. Vary, Phys. Rev. C **24**, 777 (1981); Phys Lett. **131B**, 271 (1983).
[7] K. Schmidt, University of Tubingen report, 1991.
[8] P. Ring and P. Schuck, *The Nuclear Many-Body Problem* (Springer-Verlag, New York, 1980).
[9] K. A. Brueckner, Phys. Rev. **100**, 36 (1955).
[10] K. A. Brueckner, C. A. Levinson, and H. M. Mahmoud, Phys. Rev. **95**, 217 (1954).
[11] H. A. Bethe, Phys. Rev. **103**, 1353 (1956); H. A. Bethe and J. Goldstone, Proc. R. Soc. London, Ser. A **238**, 551 (1957); J. Goldstone, *ibid.* **239**, 267 (1957).
[12] B. H. Brandow, Phys. Rev. **152**, 863 (1966); Rev. Mod. Phys. **39**, 771 (1966).
[13] A. K. Kerman, J. P. Svenne, and F. B. Villars, Phys. Rev. **147**, 710 (1966).
[14] K. T. R. Davies and R. L. Becker, Nucl. Phys. **A176**, 1 (1971).
[15] S. B. Khadkikar and V. B. Kamble, Nucl. Phys. **A225**, 352 (1974).
[16] J. P. Vary, in *Theory and Application of Moment Methods in Many-Fermion Systems*, edited by B. J. Dalton, S. M. Grimes, J. P. Vary, and S. A. Williams (Plenum, New York, 1980).
[17] R. V. Reid, Ann. Phys. (NY) **50**, 411 (1968).
[18] G. Bozzolo and J. P. Vary, Phys. Rev. C **31**, 1909 (1985).
[19] J. W. Negele, Phys. Rev. C **1**, 1260 (1970).
[20] C. W. de Jager, H. de Vries, and C. de Vries, At. Data Nucl. Data Tables **14**, 479 (1974); the "point mass" radius is 2.59 fm when the measured charge rms radius of 2.71 fm is corrected for a finite proton charge rms radius of 0.80 fm.
[21] H. Enge, *Introduction to Nuclear Physics* (Addison-Wesley, Reading, 1966).
[22] K. T. R. Davies, M. Baranger, R. M. Tarbutton, and T. T. S. Kuo, Phys Rev. **177**, 1519 (1969).
[23] L. Jaqua, M. A. Hasan, J. P. Vary, and B. R. Barrett (unpublished).
[24] T. Koopmans, Physica **1**, 104 (1943).
[25] B. R. Barrett and M. W. Kirson, in *Advances in Nuclear Physics*, edited by M. Baranger and E. Vogt (Plenum, New York, 1973), Vol. 6, p. 219; P. J. Ellis and E. Osnes, Rev. Mod. Phys. **49**, 777 (1977).
[26] J. P. Vary and S. N. Yang, Phys. Rev. C **15**, 1545 (1977).
[27] A. Etcheogoyen, W. D. M. Rae, and N. S. Godwin, OXBASH-MSU, The Oxford-Buenos Aires-Michigan State University Shell-Model Code (MSU version by B. A. Brown) (unpublished).